

INVERSE COMPTON SCATTERING  
ON LASER BEAM AND MONOCHROMATIC  
ISOTROPIC RADIATION

Daniele Fargion,<sup>1,2</sup> Rostislav V. Konoplich<sup>1,2</sup> and Andrea Salis<sup>1</sup>

<sup>1</sup> *Dipartimento di Fisica, Universita' di Roma "La Sapienza",  
P.le A. Moro 2, 00185 Rome, Italy.*

<sup>2</sup> *INFN-Sezione di Roma I, c/ o Dipartimento di Fisica,  
Universita' di Roma "La Sapienza", 00185 Rome, Italy*

**Abstract**

Most of the known literature on Inverse Compton Scattering (ICS) is based on earliest theoretical attempts and later approximations led by F.C.Jones and J.B.Blumenthal. We found an independent and more general analytical procedure which provide both *relativistic* and *ultrarelativistic* limits for ICS. These new analytical expressions can be derived in a straightforward way and they contain the previously reminded Jones' results. Our detailed solutions may be probed by already existing as well future ICS experiments.

e-mail:FARGION@ROMA1.INFN.IT

e-mail:KONOPLIC@ROSTI.MEPHI.MSK.SU

e-mail:SALIS@ROMA1.INFN.IT

Tel:39 6 4991-4287 (Fargion)

fax:4957697

## Introduction

The ICS plays a relevant role in a variety of recent high energy astrophysics (cosmic ray lifetime, gamma astronomy, gamma jets, ultrahigh energy cosmic rays (UHECR),...) as well as in high energy physics at LEP I, LEP II and linear accelerators . In particular the ICS of cosmic rays onto electromagnetic fields, either cosmological Black Body Radiation (BBR) at  $T \approx 2.73 K$  or diffused gray body as interstellar lights and radio waves or even nearly stationary magnetic fields, is source of high energy photons (X, gamma ,...) which we may observe as diffused or smeared pointlike gamma sources. The ICS onto BBR plays an important role in the complex connection between cosmic rays and gamma spectra and in the gamma burst puzzle. In this paper we derive the general ICS formulae for the interaction between a monochromatic electron beam and a monochromatic photon beam, as a laser, either unidirectional or isotropic. We shall show that our results generalize and slightly correct previous known ones [1-5]. The complexity of the ICS onto a Planckian spectrum has already been experimentally verified [6,7] as well as successfully theoretically predicted [8,9].

## The ICS on a monochromatic and unidirectional photon beam

To find the ICS spectrum we consider first the photon beam distribution in the Laboratory Frame (LF) (not to be confused with the electron rest frame EF) where this beam distribution is unidirectional and monochromatic; then we transform it in the (EF) where it still is unidirectional and monochromatic; in that frame (EF) we consider the normal Compton or Thomson scattering and finally we transform back the resulting diffused differential photon number to the LF.

Let us consider such a monochromatic and unidirectional photon beam in the LF : the differential number density per unit energy  $\epsilon_o$  and solid angle  $\Omega_o$  can be written as:

$$\frac{dn_o}{d\epsilon_o d\Omega_o} = n_o \delta(\epsilon_o - \hat{\epsilon}_o) \delta(\cos \theta_o - \cos \hat{\theta}_o) \delta(\varphi_o - \hat{\varphi}_o) \quad (1)$$

where  $\hat{\theta}_o$  is the incident angle between the electron beam and photon beam directions and  $\hat{\epsilon}_o$  is the initial photon energy in the LF. Our sources have an idealized beam with no spread both in angle and in energy. We transform now this distribution to the EF by standard Lorentz relations choosing as z axis the direction coincident with the electron momentum and reminding that  $dn_o/d\epsilon_o$  is a relativistic invariant [2]. In the following we label by a \* the quantities related to the electron frame EF, so we have

$$\cos \theta_o = \frac{\cos \theta_o^* + \beta}{1 + \beta \cos \theta_o^*}, \quad \varphi_o = \varphi_o^*, \quad \epsilon_o = \gamma \epsilon_o^* (1 + \beta \cos \theta_o^*) \quad . \quad (2)$$

where  $\beta$  is the adimensional electron velocity and  $\gamma$  is the corresponding Lorentz factor. Using  $\delta$  function properties the number density distribution, in the EF, becomes

$$\frac{dn_o^*}{d\epsilon_o^*d\Omega_o^*} = n_o\gamma(1 - \beta \cos \hat{\theta}_o) \cdot \delta[\epsilon_o^* - \gamma\hat{\epsilon}_o(1 - \beta \cos \hat{\theta}_o)]\delta[\cos \theta_o^* - \hat{C}_o]\delta(\varphi_o^* - \hat{\varphi}_o) \quad (3)$$

where  $\hat{C}_o = \theta_o^* = (\cos \hat{\theta}_o - \beta)/(1 - \beta \cos \hat{\theta}_o)$  is the function describing the boosted cosine angle  $\theta_o^*$ . Now we have to scatter and diffuse the photons in the EF; the function describing the differential number of diffused photons can be obtained as follows:

$$\frac{dN_1^*}{dt_1^*d\epsilon_1^*d\Omega_1^*d\epsilon_o^*d\Omega_o^*} = \frac{dn_o^*}{d\epsilon_o^*d\Omega_o^*} \frac{d\sigma_C}{d\epsilon_1^*d\Omega_1^*} c \quad (4)$$

where  $\frac{d\sigma_C}{d\epsilon_1^*d\Omega_1^*}$  is the Klein-Nishina differential cross section

$$\frac{d\sigma_C}{d\epsilon_1^*d\Omega_1^*} = \frac{r_o^2}{2} \left( \frac{\epsilon_1^*}{\epsilon_o^*} \right)^2 \left( \frac{\epsilon_1^*}{\epsilon_o^*} + \frac{\epsilon_o^*}{\epsilon_1^*} - \sin^2 \theta_{sc}^* \right) \delta \left( \epsilon_1^* - \frac{\epsilon_o^*}{1 + \epsilon_o^*(1 - \cos \theta_{sc}^*)/mc^2} \right) .$$

For most of the real ICS processes in present laboratories energetics it is possible to approximate the Klein-Nishina cross section by the Thomson cross section, *i.e.*  $\epsilon_o^* \ll mc^2$ , so we can consider

$$\frac{d\sigma_T}{d\epsilon_1^*d\Omega_1^*} = \frac{r_o^2}{2} (1 + \cos^2 \theta_{sc}^*) \delta(\epsilon_1^* - \epsilon_o^*) \quad (5)$$

where  $c$  is the speed of light. The dependence of  $\sigma_T$  by the inverse square electron mass leads us to consider mainly electron bunches. However our results can be applied also to protons where we have just a suppression factor  $(m_e/m_p)^2$ . The scattering angle in the EF must be expressed as a function of the other angles involved, *i.e.* the incoming  $\theta_o^*, \varphi_o^*$  and the outgoing  $\theta_1^*, \varphi_1^*$  angles

$$\cos \theta_{sc}^* = \sin \theta_o^* \sin \theta_1^* (\cos \varphi_o^* \cos \varphi_1^* + \sin \varphi_o^* \sin \varphi_1^*) + \cos \theta_o^* \cos \theta_1^* \quad . \quad (6)$$

It is interesting to notice that the distribution number  $\frac{dN_1}{dt_1^*d\epsilon_1^*d\Omega_1^*}$  cannot be associated to any effective number density because of its intrinsic inhomogeneous nature. Finally we obtain the differential photon number per unit energy and solid angle in the LF by the inverse Lorentz transformations and we write it in the following integral form:

$$\frac{dN_1}{dt_1 d\epsilon_1 d\Omega_1} = \int_{\Omega_o^*} \int_{\epsilon_o^*} \frac{dN_1^*}{dt_1^* d\epsilon_1^* d\Omega_1^* d\epsilon_o^* d\Omega_o^*} \frac{dt_1^*}{dt_1} \frac{d\epsilon_1^*}{d\epsilon_1} \frac{d\Omega_1^*}{d\Omega_1} d\Omega_o^* d\epsilon_o^* \quad . \quad (7)$$

By substitution of previous eqs.(4,6) and since  $\frac{dt_1^*}{dt_1} \frac{d\epsilon_1^*}{d\epsilon_1} \frac{d\Omega_1^*}{d\Omega_1} = \frac{1}{\gamma^2(1-\beta \cos \theta_1)}$  the integral can be cast into the form

$$\frac{dN_1}{dt_1 d\epsilon_1 d\Omega_1} = \frac{n_o r_o^2 c (1 - \beta \cos \hat{\theta}_o)}{2\gamma (1 - \beta \cos \theta_1)} \int_{\epsilon_o^*} \int_{\Omega_o^*} (1 + \cos^2 \theta_{sc}^*) \delta(\epsilon_1^* - \epsilon_o^*) \cdot$$

$$\cdot \delta[\epsilon_o^* - \gamma \hat{\epsilon}_o(1 - \beta \cos \hat{\theta}_o)] \delta(\cos \theta_o^* - \hat{C}_o) \delta(\varphi_o^* - \hat{\varphi}_o) d\epsilon_o^* d\Omega_o^* \quad . \quad (8)$$

We perform the integrals and the final form for the differential photon number per unit energy and solid angle in the Laboratory Frame becomes

$$\begin{aligned} \frac{dN_1}{dt_1 d\epsilon_1 d\Omega_1} &= \frac{n_o r_o^2 c}{2\beta \gamma^2 \epsilon_1} \frac{(1 - \beta \cos \hat{\theta}_o)}{(1 - \beta \cos \theta_1)} \left( 1 + C_1^2 \hat{C}_o^2 + (1 - C_1^2)(1 - \hat{C}_o^2)(\cos \varphi_1 \cos \hat{\varphi}_o + \right. \\ &+ \left. \sin \varphi_1 \sin \hat{\varphi}_o)^2 + 2C_1 \hat{C}_o (1 - C_1^2)^{1/2} (1 - \hat{C}_o^2)^{1/2} (\cos \varphi_1 \cos \hat{\varphi}_o + \sin \varphi_1 \sin \hat{\varphi}_o) \right) \cdot \\ &\cdot \delta \left[ \cos \theta_1 - \frac{1}{\beta} \left( 1 - \frac{\hat{\epsilon}_o}{\epsilon_1} (1 - \beta \cos \hat{\theta}_o) \right) \right] \quad . \quad (9) \end{aligned}$$

where  $C_1 = \cos \theta_1^* = (\cos \theta_1 - \beta)/(1 - \beta \cos \theta_1)$ . The final ICS spectrum can be obtained by integrating over  $\Omega_1$  the previous equation and the result is:

$$\frac{dN_1}{dt_1 d\epsilon_1} = \frac{\pi n_o r_o^2 c}{2\beta \gamma^2 \hat{\epsilon}_o} \left[ 3 - \hat{C}_o^2 + (3\hat{C}_o^2 - 1) \frac{1}{\beta^2} \left( \frac{\epsilon_1}{\gamma^2 \hat{\epsilon}_o (1 - \beta \cos \hat{\theta}_o)} - 1 \right)^2 \right]. \quad (10)$$

Let us notice that this energy distribution does not depend on the initial azimuthal angle  $\hat{\varphi}_o$  due to the axial symmetry of the problem. The  $\epsilon_1$  dependence shows that the original monochromatic and unidirectional photon spectrum has been spread into a final parabolic function. We show below its behaviour for some arbitrary parameters (fig.1-5). The spectrum is bound in energy by relativistic kinematics arguments and its extreme  $\epsilon_1$  allowed values are  $\epsilon_{1min} = \hat{\epsilon}_o(1 - \beta \cos \hat{\theta}_o)/(1 + \beta)$  and  $\epsilon_{1max} = \hat{\epsilon}_o(1 - \beta \cos \hat{\theta}_o)/(1 - \beta)$ . The  $\theta_1$  angle is simply varying into the range  $[0, \pi]$  and, as usual, the most populate angular region of the high energy ICS beam is contained inside a thin cone whose aperture is of order  $1/\gamma$ . If we substitute in eq.(10)  $\epsilon_{1min}$  and  $\epsilon_{1max}$  we get an equal height for the parabolic spectrum extremes:

$$\frac{dN_1}{dt_1 d\epsilon_1 |_{\epsilon_1(min,max)}} = \frac{\pi n_o r_o^2 c}{\beta \gamma^2 \hat{\epsilon}_o} [1 + \hat{C}_o^2] \quad . \quad (11)$$

The spectrum has a minimum for  $\epsilon_1 = \gamma^2 \hat{\epsilon}_o (1 - \beta \cos \hat{\theta}_o)$  and in this point its value is:

$$\frac{dN_1}{dt_1 d\epsilon_1 |_{min}} = \frac{\pi n_o r_o^2 c}{2\beta \gamma^2 \hat{\epsilon}_o} [3 - \hat{C}_o^2] \quad . \quad (12)$$

The above expressions are the rigorous analytical spectra for Thomson ICS onto a monochromatic and unidirectional photon beam. From eq.(9) we can also get the angular distribution of scattered photons and the total rate number:

$$\begin{aligned} \frac{dN_1}{dt_1 d\Omega_1} &= \frac{n_o r_o^2 c}{2\gamma^2} \frac{(1 - \beta \cos \hat{\theta}_o)}{(1 - \beta \cos \theta_1)^2} [1 + C_1^2 \hat{C}_o^2 + (1 - C_1^2)(1 - \hat{C}_o^2)(\cos \varphi_1 \cos \hat{\varphi}_o + \\ &+ \sin \varphi_1 \sin \hat{\varphi}_o)^2 + 2C_1 \hat{C}_o (1 - C_1^2)^{1/2} (1 - \hat{C}_o^2)^{1/2} (\cos \varphi_1 \cos \hat{\varphi}_o + \sin \varphi_1 \sin \hat{\varphi}_o)] \quad (13) \end{aligned}$$

and

$$\frac{dN_1}{dt_1} = \sigma_T n_o c (1 - \beta \cos \hat{\theta}_o) \quad . \quad (14)$$

The spectrum in eq.(10) may be tested on known records of ICS. Our eq.(10) also contains the non relativistic limit where, for  $\beta \rightarrow 0$ , one must recover the correct initial Dirac delta function  $\delta(\epsilon_1 - \hat{\epsilon}_o)$ .

### ICS on a monochromatic and unidirectional electron beam beyond the Thomson limit

Let us consider now the ICS in the framework of quantum electrodynamics in order to obtain the exact Compton result for the corresponding particle distribution in the case of a monochromatic and unidirectional photon beam. Considering two Feynman diagrams which contribute to this process the standard calculations give us the following expressions for the matrix element (in this section we use  $\hbar = c = 1$ ):

$$|\bar{M}|^2 = 2^5 \pi^2 r_o^2 m^2 \left( \left[ m^2 \left( \frac{1}{\kappa_o p_o} - \frac{1}{\kappa_1 p_o} \right) + 1 \right]^2 + \frac{\kappa_1 p_o}{\kappa_o p_o} + \frac{\kappa_o p_o}{\kappa_1 p_o} - 1 \right) \quad (15)$$

where  $\kappa_o p_o = \hat{\epsilon}_o m \gamma (1 - \beta \cos \hat{\theta}_o)$ ,  $\kappa_1 p_o = \epsilon_1 m \gamma (1 - \beta \cos \theta_1)$ . The corresponding cross section is given by

$$d\sigma = \frac{1}{2^6 \pi^2} \frac{|\bar{M}|^2}{(p_o \kappa_o)} \delta^{(4)}(p_o + \kappa_o - p_1 - \kappa_1) \frac{d^3 \kappa_1}{\epsilon_1} \frac{d^3 p_1}{E_1} \quad . \quad (16)$$

In the case of colliding beams the number of collisions per second can be obtained from the following relation

$$d\dot{N}_1 = L d\sigma \quad (17)$$

where L is the luminosity which is defined by [10]

$$L = n_o n_1 V (1 - \beta \cos \hat{\theta}_o) \quad (18)$$

V is the unit volume in the LF. In our case  $n_1 V = 1$ , the density  $n_o$  was defined in eq.(1). Now integrating eq.16 over the corresponding variables we obtain the following exact expression for the angular distribution of scattered photons:

$$\frac{dN_1}{dt_1 d\Omega_1} = n_o \frac{r_o^2}{2} \frac{m^2 \epsilon_1^2}{(p_o \kappa_o)^2} (1 - \beta \cos \hat{\theta}_o) \cdot \left( \left[ m^2 \left( \frac{1}{\kappa_o p_o} - \frac{1}{\kappa_1 p_o} \right) + 1 \right]^2 + \frac{\kappa_1 p_o}{\kappa_o p_o} + \frac{\kappa_o p_o}{\kappa_1 p_o} - 1 \right) \quad (19)$$

where

$$\epsilon_1 = \frac{\hat{\epsilon}_o m \gamma (1 - \beta \cos \hat{\theta}_o)}{\gamma m (1 - \beta \cos \theta_1) + \hat{\epsilon}_o (1 - \cos \theta_{sc})}$$

and the scattering angle is defined as in eq.(6) but in the LF. The energy spectrum of ICS is given by

$$\begin{aligned}
\frac{dN_1}{dt_1 d\epsilon_1} = & n_o \pi r_o^2 \frac{m}{\hat{\epsilon}_o \gamma} \left( \frac{\gamma m^5}{\hat{\epsilon}_o^2 A^{3/2}} [\epsilon_1 (\hat{\epsilon}_o + m\gamma\beta \cos \hat{\theta}_o) + \right. \\
& + \beta (\hat{\epsilon}_o \cos \hat{\theta}_o + m\gamma\beta) (m\gamma(1 - \beta \cos \hat{\theta}_o) - \epsilon_1)] + \frac{\kappa_o p_o}{\hat{\epsilon}_o A^{1/2}} \left[ 1 - \frac{2m^2}{\kappa_o p_o} - 2 \left( \frac{m^2}{\kappa_o p_o} \right)^2 \right] + \\
& + \frac{1}{B^{1/2}} \left[ \left( \frac{m^2}{\kappa_o p_o} \right)^2 + \frac{2m^2}{\kappa_o p_o} + \frac{\epsilon_1 \gamma m}{\kappa_o p_o} \right] + \frac{m\gamma\beta}{(\kappa_o p_o) B^{3/2}} (\hat{\epsilon}_o \cos \hat{\theta}_o + m\gamma\beta) \cdot \\
& \left. \cdot (\kappa_o p_o - \epsilon_1 \gamma m - \epsilon_1 \hat{\epsilon}_o) \right) \quad (20)
\end{aligned}$$

where

$$\begin{aligned}
A = & m^2 \left( \gamma^2 [m\gamma\beta(1 - \beta \cos \hat{\theta}_o) + \epsilon_1 (\cos \hat{\theta}_o - \beta)]^2 + \epsilon_1^2 (1 - \cos^2 \hat{\theta}_o) \right) \\
B = & \hat{\epsilon}_o^2 + m^2 \gamma^2 \beta^2 + 2\hat{\epsilon}_o m\gamma\beta \cos \hat{\theta}_o
\end{aligned}$$

and

$$\frac{\hat{\epsilon}_o m\gamma(1 - \beta \cos \hat{\theta}_o)}{m\gamma + \hat{\epsilon}_o + \sqrt{B}} \leq \epsilon_1 \leq \frac{\hat{\epsilon}_o m\gamma(1 - \beta \cos \hat{\theta}_o)}{m\gamma + \hat{\epsilon}_o - \sqrt{B}}$$

These exact expressions reproduce and confirm all the results of previous section as Thomson limit cases. Therefore eq.(10) can be used for further calculations of ICS on an isotropic monoenergetic background within the Thomson limit. Expression (20) may find application when considering the most energetic accelerators where the colliding electron and photon beams are of high energy. The behaviour of the analytical formula eq.(20) is shown in fig.6. In comparison with the spectrum discussed above we note that the Thomson "parabolic" behaviour becomes in the present Compton case an asymmetric curve which (in extreme ultrarelativistic regime where  $\hat{\epsilon}_o \gamma \gg m$ ) leads asymptotically to a nearly peaked curve at energy  $\epsilon_1 \simeq m\gamma$ .

## The ICS onto a monochromatic and isotropic photon spectrum

In ref.[2] F.C. Jones found the ultrarelativistic ICS spectrum resulting from the interaction between high energy electrons and an isotropic and monochromatic photon spectrum. We show that his result can be obtained and slightly corrected by integrating eq.(10) over all permitted  $\hat{\theta}_o$  angles. Our analytical and exact result can be set in a very compact form and it is derived from the following integral

$$\frac{dN_{1is}}{dt_1 d\epsilon_1} = \frac{1}{4\pi} \int_{\Omega_o} \frac{dN_1}{dt_1 d\epsilon_1} d\Omega_o =$$

$$= \frac{\pi n_o r_o^2 c}{4\beta\gamma^2\hat{\epsilon}_o} \int_{\hat{\theta}_{min}}^{\hat{\theta}_{max}} \left[ 3 - \hat{C}_o^2 + (3\hat{C}_o^2 - 1) \frac{1}{\beta^2} \left( \frac{\epsilon_1}{\gamma^2\hat{\epsilon}_o(1 - \beta \cos \hat{\theta}_o)} - 1 \right)^2 \right] \sin \hat{\theta}_o d\hat{\theta}_o \quad (21)$$

The upper and lower limits of this integral can be found from the inequality  $\epsilon_{1min} \leq \epsilon_1 \leq \epsilon_{1max}$  where the minimum and maximum energies of scattered photons were defined in the first section. Thus we obtain

$$\begin{aligned} \frac{1 - \beta}{1 + \beta} \hat{\epsilon}_o \leq \epsilon_1 \leq \hat{\epsilon}_o & \quad \frac{1}{\beta} \left[ 1 - \frac{\epsilon_1}{\hat{\epsilon}_o} (1 + \beta) \right] \leq \cos \hat{\theta}_o \leq 1 \\ \hat{\epsilon}_o \leq \epsilon_1 \leq \frac{1 + \beta}{1 - \beta} \hat{\epsilon}_o & \quad -1 \leq \cos \hat{\theta}_o \leq \frac{1}{\beta} \left[ 1 - \frac{\epsilon_1}{\hat{\epsilon}_o} (1 - \beta) \right] . \end{aligned}$$

As one can see from these expressions only photons incoming within a thin cone in the direction of the electron beam contribute to the lowest energy final photons meanwhile photons moving in the opposite direction contribute to the highest energy part of the spectrum. An elementary calculation gives

$$\begin{aligned} \frac{dN_{1is}}{dt_1 d\epsilon_1} = \frac{\pi n_o r_o^2 c}{4\beta^4 \gamma^2 \hat{\epsilon}_o} & \left( \left[ 3\beta^2 - 2 + \frac{3}{\beta^2} \right] x + \frac{2}{\gamma^2} \left[ \left( 1 - \frac{3}{\beta^2} \right) \left( 1 + \frac{\epsilon_1}{\hat{\epsilon}_o} \right) \right] \ln x + \right. \\ & + \frac{1}{\gamma^4} \left[ \left( 1 - \frac{3}{\beta^2} \right) \left( 1 + \frac{\epsilon_1^2}{\hat{\epsilon}_o^2} \right) - \frac{12\epsilon_1}{\beta^2 \hat{\epsilon}_o} \right] \frac{1}{x} + \\ & \left. + \frac{3\epsilon_1}{\beta^2 \gamma^6 \hat{\epsilon}_o} \left( 1 + \frac{\epsilon_1}{\hat{\epsilon}_o} \right) \frac{1}{x^2} - \frac{\epsilon_1^2}{\beta^2 \gamma^8 \hat{\epsilon}_o^2} \frac{1}{x^3} \right)_{x_{min}}^{x_{max}} \quad (22) \end{aligned}$$

where  $x = (1 - \beta \cos \hat{\theta}_o)$ . We have now two different regions depending on the value assumed by the ratio  $\epsilon_1/\hat{\epsilon}_o$ : if  $\frac{(1-\beta)\hat{\epsilon}_o}{1+\beta} \leq \epsilon_1 \leq \hat{\epsilon}_o$  then  $x_{max} = [\epsilon_1(1+\beta)/\hat{\epsilon}_o]$  and  $x_{min} = (1 - \beta)$ ; if  $\hat{\epsilon}_o \leq \epsilon_1 \leq \frac{(1+\beta)\hat{\epsilon}_o}{1-\beta}$  then  $x_{max} = (1 + \beta)$ ,  $x_{min} = [\epsilon_1(1 - \beta)/\hat{\epsilon}_o]$ . The two separate formulae, left and right, must vanish respectively at  $\epsilon_1 = \hat{\epsilon}_o(1 - \beta)/(1 + \beta)$  and  $\epsilon_1 = \hat{\epsilon}_o(1 + \beta)/(1 - \beta)$  and they must obviously coincide for  $\epsilon_1 = \hat{\epsilon}_o$ . Labelling by L the left hand side and by R the right hand side, with respect to the value  $\epsilon_1 = \hat{\epsilon}_o$ , the two formulae, exact in the whole range of allowable values for the ratio  $\epsilon_1/\hat{\epsilon}_o$ , become

$$\begin{aligned} \frac{dN_{1is L}}{dt_1 d\epsilon_1} = \frac{\pi n_o r_o^2 c}{4\beta^6 \gamma^2 \hat{\epsilon}_o} & \left( \frac{\epsilon_1}{\hat{\epsilon}_o} (1 + \beta) \left[ \beta(\beta^2 + 3) + \frac{1}{\gamma^2} (9 - 4\beta^2) \right] + \right. \\ & + (1 - \beta) \left[ \beta(\beta^2 + 3) - \frac{1}{\gamma^2} (9 - 4\beta^2) \right] + \\ & \left. - \frac{2}{\gamma^2} (3 - \beta^2) \left( 1 + \frac{\epsilon_1}{\hat{\epsilon}_o} \right) \ln \left[ \frac{\epsilon_1(1 + \beta)}{\hat{\epsilon}_o(1 - \beta)} \right] - \frac{\hat{\epsilon}_o}{\gamma^4 \epsilon_1} + \frac{\epsilon_1^2}{\gamma^4 \hat{\epsilon}_o^2} \right) \quad (23a) \end{aligned}$$

and

$$\frac{dN_{1is R}}{dt_1 d\epsilon_1} = \frac{\pi n_o r_o^2 c}{4\beta^6 \gamma^2 \hat{\epsilon}_o} \left( (1 + \beta) \left[ \beta(\beta^2 + 3) + \frac{1}{\gamma^2} (9 - 4\beta^2) \right] + \right.$$

$$\begin{aligned}
& + \frac{\epsilon_1}{\hat{\epsilon}_o}(1 - \beta) \left[ \beta(\beta^2 + 3) - \frac{1}{\gamma^2}(9 - 4\beta^2) \right] + \\
& - \frac{2}{\gamma^2}(3 - \beta^2) \left( 1 + \frac{\epsilon_1}{\hat{\epsilon}_o} \right) \ln \left[ \frac{\hat{\epsilon}_o(1 + \beta)}{\epsilon_1(1 - \beta)} \right] + \frac{\hat{\epsilon}_o}{\gamma^4 \epsilon_1} - \frac{\epsilon_1^2}{\gamma^4 \hat{\epsilon}_o^2} \Big) . \quad (23b)
\end{aligned}$$

We notice that the two expressions exhibit some kind of symmetry, in particular the second one can be obtained from the first one simply by reversing the  $\beta$  sign and multiplying the whole formula by (-1). The non relativistic limit  $\beta \rightarrow 0$  in eq.(23a,b) leads to a monochromatic spectrum, *i.e.* a Dirac  $\delta$  function, as it should be expected. Now we consider the ultrarelativistic limit  $\beta \rightarrow 1$  and, neglecting terms smaller than  $1/\gamma^2$  we get

$$\frac{dN_{1is\ L}}{dt_1 d\epsilon_1} \approx \frac{\pi n_o r_o^2 c}{2\gamma^4 \hat{\epsilon}_o \beta^6} \left[ (4\gamma^2 + 2) \frac{\epsilon_1}{\hat{\epsilon}_o} + 1 - \frac{3}{2\gamma^2} - 2 \left( 1 + \frac{\epsilon_1}{\hat{\epsilon}_o} \right) \ln \left( \frac{4\gamma^2 \epsilon_1}{\hat{\epsilon}_o} \right) - \frac{\hat{\epsilon}_o}{2\gamma^2 \epsilon_1} \right] \quad (24a)$$

for  $\frac{1}{4\gamma^2} < \frac{\epsilon_1}{\hat{\epsilon}_o} \leq 1$  and

$$\frac{dN_{1is\ R}}{dt_1 d\epsilon_1} \approx \frac{\pi n_o r_o^2 c}{2\gamma^4 \hat{\epsilon}_o \beta^6} \left[ 4\gamma^2 + 2 + \left( 1 - \frac{3}{2\gamma^2} \right) \frac{\epsilon_1}{\hat{\epsilon}_o} - 2 \left( 1 + \frac{\epsilon_1}{\hat{\epsilon}_o} \right) \ln \left( \frac{4\gamma^2 \hat{\epsilon}_o}{\epsilon_1} \right) - \frac{\epsilon_1^2}{2\gamma^2 \hat{\epsilon}_o^2} \right] . \quad (24b)$$

for  $1 \leq \frac{\epsilon_1}{\hat{\epsilon}_o} < 4\gamma^2$ . These equations must be compared with eq.(40) and eq.(44) of ref.[2]. We note that we have a slight difference in a couple of terms and in the coefficient in front of the logarithmic term. From inspection of fig.7-8 one sees that Jones' approximated formulae exhibit a slight departure from our exact expressions and the difference is of order  $1/\gamma^2$ . Moreover it is also possible to notice that our eq.24 represent a better approximation for most of the  $\epsilon_1/\hat{\epsilon}_o$  allowed values. At ultrarelativistic regime all the three kinds of expressions (eq.23, eq.24, Jones' approximations) are overlapping. For most applications where both non relativistic and ultrarelativistic regimes are of interest we consider our exact formula (23) which is more convenient to handle than the Jones' significantly more complicated expression eq.(35) in ref.[2].

## Conclusions

We derived exact analytical formulae able to describe the ICS onto monochromatic beam lasers either in relativistic and non relativistic limits. Our results correct and extend previous known ones. These new formulae are to prefer because of their straightforward derivation and their more transparent form. As we have already shown in a separate paper [11] our results on ICS onto BBR successfully fit the known experimental data taken at LEP I in recent years. This process, ICS onto BBR, plays an important role also in astrophysical problems where the cosmic rays energy loss by ICS and its consequent ICS radiation in gamma rays is of primary relevance. ICS onto stellar BBR may also be important in solving the well known GRB puzzle. We also



note that the coherent nature of ICS process may significantly amplify the ICS itself offering a powerful diagnostic tool for the distribution of charges in the bunch. The optimal experimental setup should be realized when relativistic bunches of charges are hit by collinear back photon lasers at optical or infrared wavelengths.

## Acknowledgements

We wish to thank Dott. L.Silvestrini for useful comments.

## References

- [1] V.L.Ginzburg, S.I.Syrovatskii, Soviet Phys.JETP 19 (1964) 1255.
- [2] F.C.Jones, Phys.Rev. 167 (1968) 1159.
- [3] G.R.Blumenthal, R.J.Gould, Rev.Mod.Phys. 42 (1970) 237.
- [4] M.S.Longair, High Energy Astrophysics (Cambridge University Press, 1981).
- [5] V.S.Berezinskii, S.V.Bulanov, V.A.Dogiel, V.L.Ginzburg, V.S. Ptuskin, Astrophysics of Cosmic Rays (North Holland, 1990).
- [6] B.Dehning, A.C.Melissinos, P.Ferrone, C.Rizzo, G.von Holtey, Phys.Lett.B 249 (1990) 145.
- [7] C.Bini, G.De Zorzi, G.Diambri-Palazzi, G.Di Cosimo, A.Di Domenico, P.Gauzzi, D.Zanello, Phys.Lett.B 262 (1991) 135.
- [8] A.Di Domenico, Particle Accelerators 39 (1992) 137.
- [9] D.Fargion, A.Salis, Nucl.Phys.B (Proc.Suppl.) 43 (1995) 269.
- [10] E.Segre', Nuclei e Particelle (Zanichelli, 1994) p.137.
- [11] D.Fargion, A.Salis, Preprint INFN n.1134 23/02/96, submitted to New Astronomy

### Figure Captions

- **Fig.1:** The energy spectrum (eq.10) for  $\hat{\theta}_o = 0$  (dash),  $\hat{\theta}_o = \pi/2$  (dot),  $\hat{\theta}_o = \pi$  (continuous)
- **Fig.2:** The energy spectrum (eq.10) for  $\hat{\theta}_o = 0$  and  $\gamma = 10$  (dash),  $\gamma = 100$  (dot),  $\gamma = 1000$  (continuous)
- **Fig.3:** The energy spectrum (eq.10) for  $\hat{\theta}_o = \pi/2$  and  $\gamma = 10$  (dash),  $\gamma = 100$  (dot),  $\gamma = 1000$  (continuous)
- **Fig.4:** The energy spectrum (eq.10) for  $\hat{\theta}_o = \pi$  and  $\gamma = 10$  (dash),  $\gamma = 100$  (dot),  $\gamma = 1000$  (continuous)
- **Fig.5:** The energy spectrum (eq.10) for  $\hat{\theta}_o = \pi/2$ ,  $\gamma = 100$  and  $\hat{\epsilon}_o = 1 eV$  (dash),  $\hat{\epsilon}_o = 0.1 eV$  (dot),  $\hat{\epsilon}_o = 0.01 eV$  (continuous)
- **Fig.6:** The energy spectrum (eq.20) for  $\hat{\theta}_o = \pi$ ,  $\gamma = 10^6$  and  $\hat{\epsilon}_o = 10^{-8} MeV$  (parabolic curve),  $\hat{\epsilon}_o = 10^{-6} MeV$  (asymmetric parabolic curve),  $\hat{\epsilon}_o = 10^{-4} MeV$  (peaked curve)
- **Fig.7:** The exact spectrum (eq.23) (continuous) and the approximations: Jones' (eq.40-44) (dash), eq.(24) (dot) for  $\gamma = 2$
- **Fig.8:** The exact spectrum (eq.23) (continuous) and the approximations: Jones' (eq.40-44) (dash), eq.(24) (dot) for  $\gamma = 5$

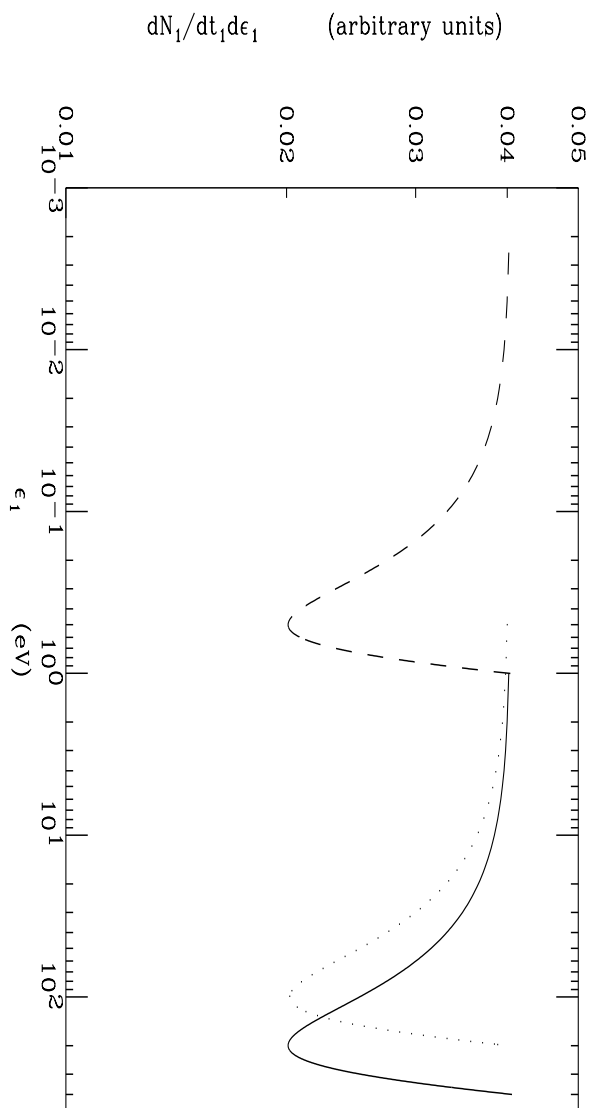


Figure 1:

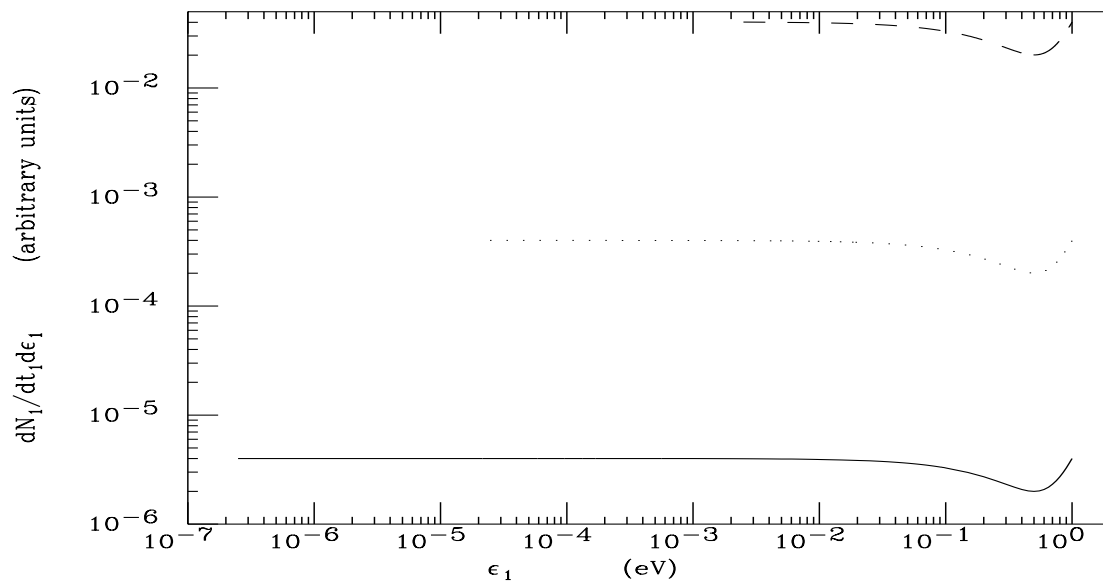


Figure 2:

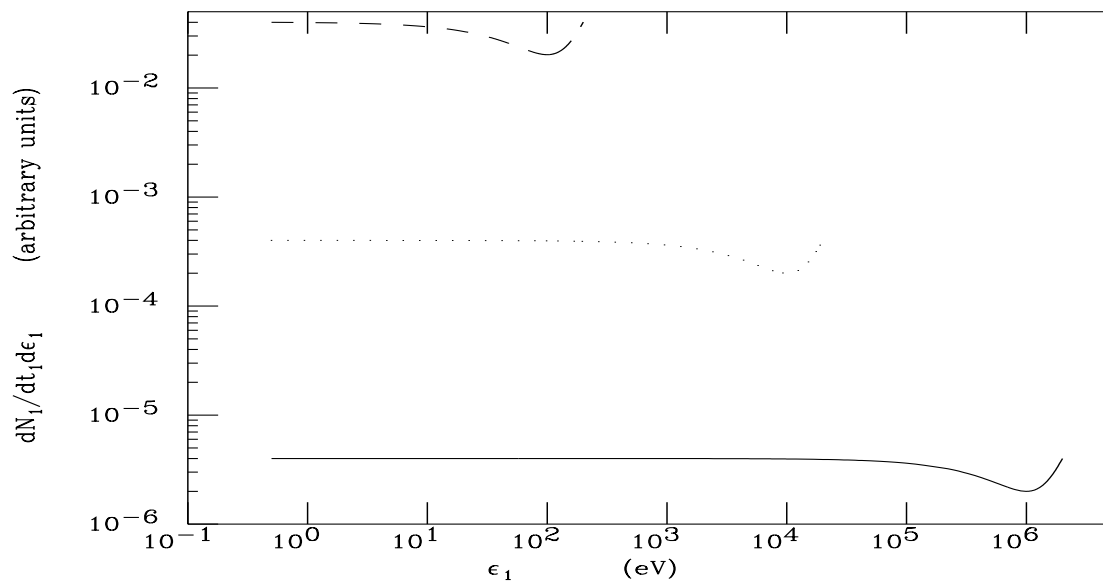


Figure 3:

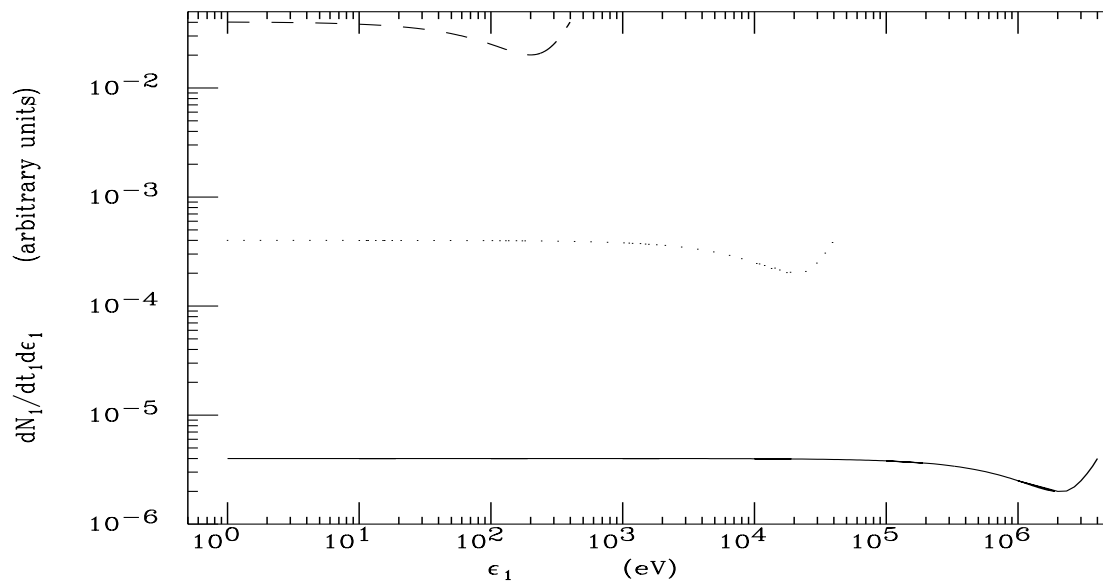


Figure 4:

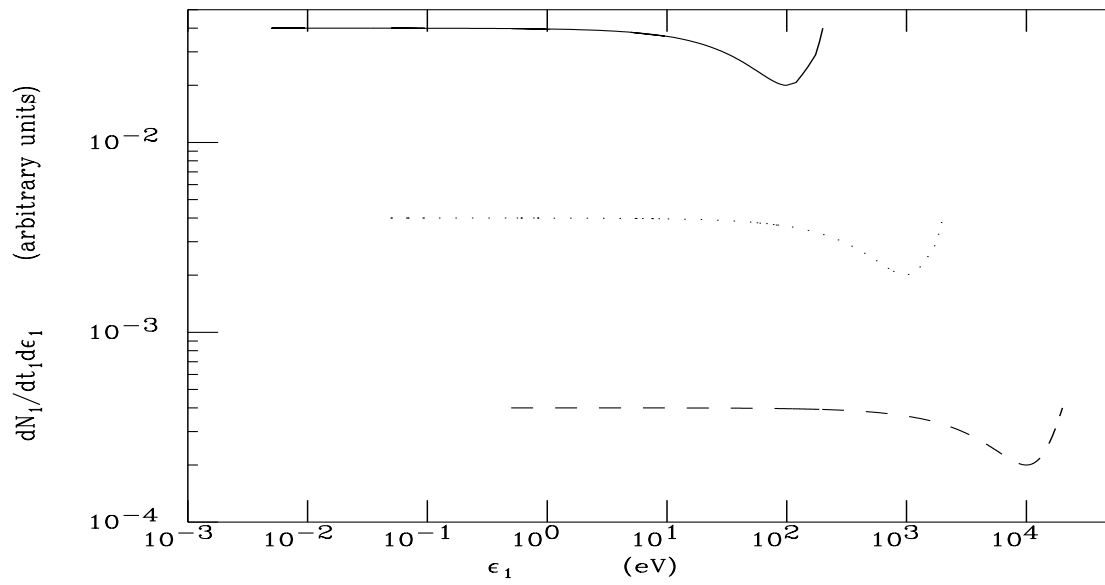


Figure 5:

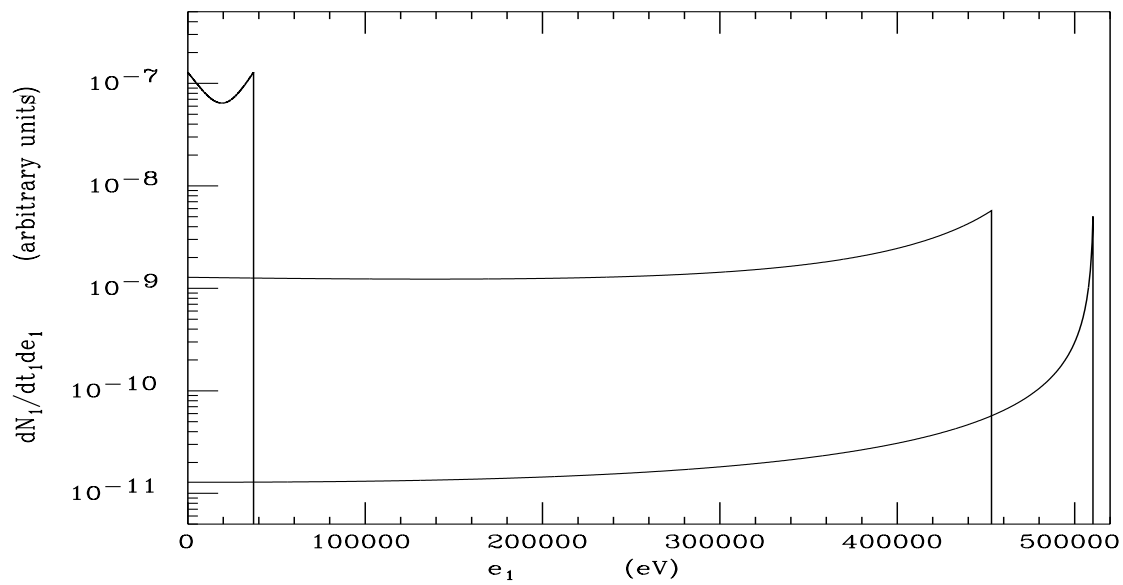


Figure 6:



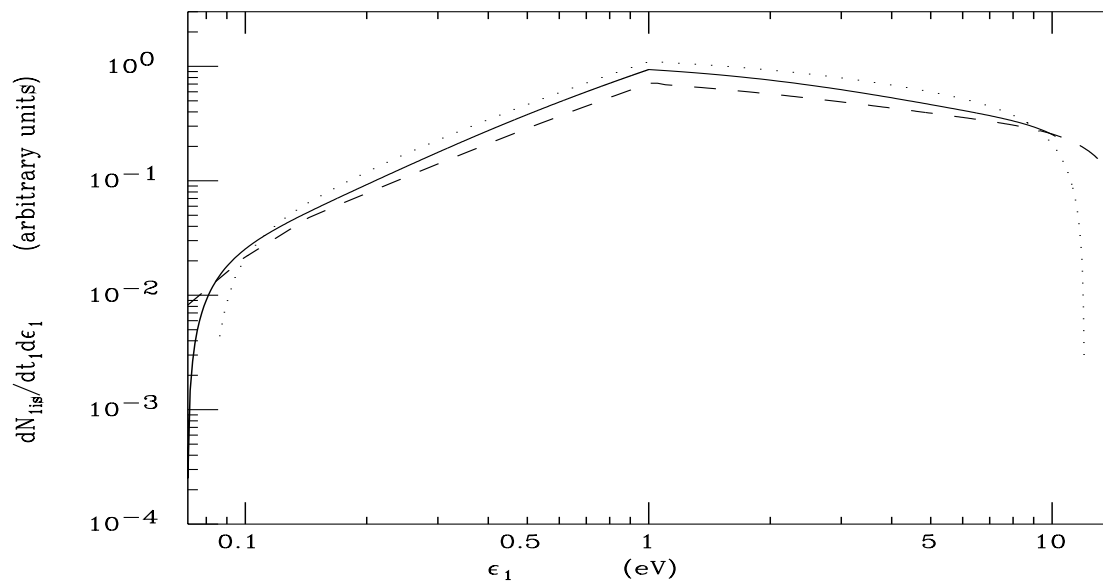


Figure 7:

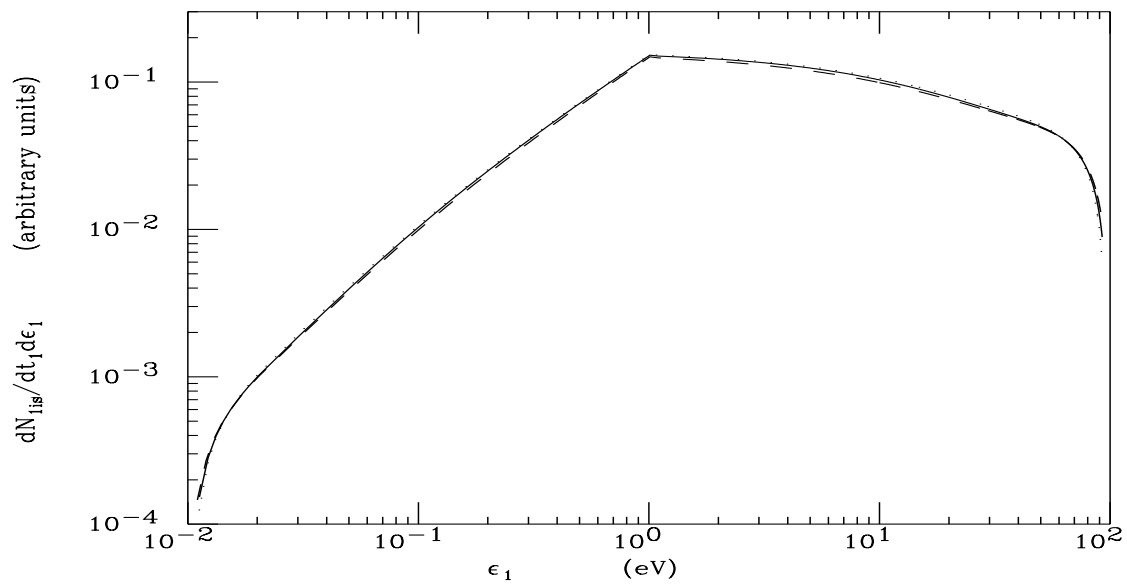


Figure 8: